K-8-4(Invited)

Extended Abstracts of the 2009 International Conference on Solid State Devices and Materials, Sendai, 2009, pp1402-1403

Spin Injection, Transport, and Control in Silicon and near the Si/SiO_2 interface

Ian Appelbaum
Center for Nanophysics and Advanced Materials and Department of Physics,
University of Maryland, College Park MD 20742 USA
Phone: (301) 405-0890 E-mail: appelbaum@physics.umd.edu

I. INTRODUCTION

Electrons have fundamental electric charge, mass, and magnetic moment associated with intrinsic angular momentum called "spin". In today's semiconductor devices, electron spin orientation is random and its effects can be ignored. However, spin polarized electron currents can be used to make novel "spintronic" devices with unusual functionality or performance.

To integrate this semiconductor spintronics into current MOSFET technology, it is important to realize lateral spin transport in silicon and study it near the semiconductor/oxide interface as well as in bulk[1]. Previously, we have performed the first experimental studies of long-distance vertical spin transport devices[1, 2], and lateral spin transport in silicon has been demonstrated even over 2mm distance[3]. However, this has been done in a quasi-lateral geometry with a significant vertical component to the transport direction. In this study, we have realized true lateral spin transport in silicon using hot electron injection/detection techniques and demonstrated it with clear spin rotation (precession) signals as well as spin valve measurements. Furthermore, we have investigated spin transport near the interface of silicon/silicon dioxide with an electrostatic gate.

II. DEVICE FABRICATION

To fabricate the device, we used ultra-high vacuum metal film wafer bonding to assemble a semiconductor-metal-semiconductor hot-electron spin detector; two different silicon-on insulator (SOI) wafers, one with a 10μm single-crystal (100) undoped silicon layer and the other with a 3μm phosphorous doped n-type layer, were bonded together with a $Ni_{80}Fe_{20}$ (4nm)/ Cu (4nm) bilayer. Both wafers have a 1μm thick thermally-oxidized SiO_2 layer as a buried insulator. Then, the detector composed of the 3μm n-type silicon layer was patterned and the 10μm undoped silicon transport layer was exposed by conventional photolithography and wet-etching. Ar^+ ion milling was used to remove any residual metal silicide formed at and under the surface of the 10μm undoped silicon spin transport layer[4]. A hot-electron spin injector was built with a ferromagnetic emitter oxide tunnel junction, Al (40nm)/$Co_{84}Fe_{16}$ (10nm)/Al_2O_3/Al (5nm)/Cu (5nm) on the 10μm i-Si layer, approximately 200 μm from the detector. A schematic of our device structure is illustrated in Fig. 1.

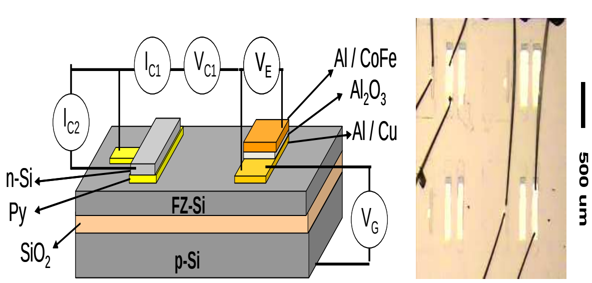

FIG. 1: Schematic of device structure (left) and top view photo of wire-bonded devices (right).

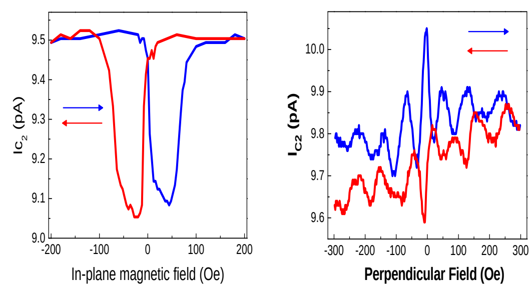

FIG. 2: Spin-valve (left) and spin precession measurements (right) at 45 K with V_G = 6V, V_{C1} = 8V, and V_E = -1.7V

III. MEASUREMENT RESULTS

To confirm lateral spin transport in our silicon device, the spin signal collector 2 current (I_{C2}) was measured applying an external magnetic field parallel to the transport layer (spin-valve effect) and perpendicular to the layer as well (to induce spin precession), as shown in Fig. 2. Clear oscillations due to spin precession confirm the realization of lateral spin transport in Silicon. Fig. 3 displays the magneto-current (MC) ratio $(I_{C2}^{P} - I_{C2}^{AP})/I_{C2}^{AP}$, where the superscripts refer to parallel and antiparallel injector/detector magnetization configuration, respectively, with various values of accelerating voltage V_{C1} and gate voltage V_G at temperature 45K and emitter voltage V_E = - 1.7V; as V_{C1} increases, MC increases until it saturates. However, as V_G increases and electrons are attracted to the interface of Si/SiO_2), MC decreases significantly. In Fig. 4, average spin transit time τ is calculated using π rad precession minima field values Bπ measured

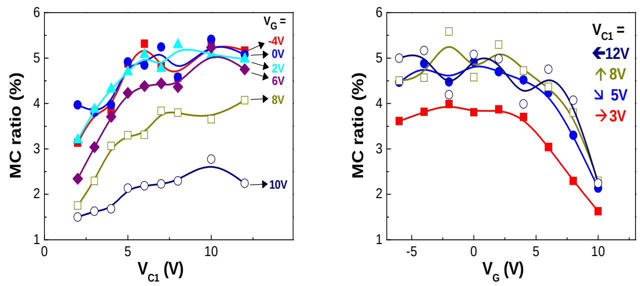

FIG. 3: Magneto-current (MC) ratio versus V_{C1} (left) and V_G (right) at T = 45K and V_E = -1.7V.

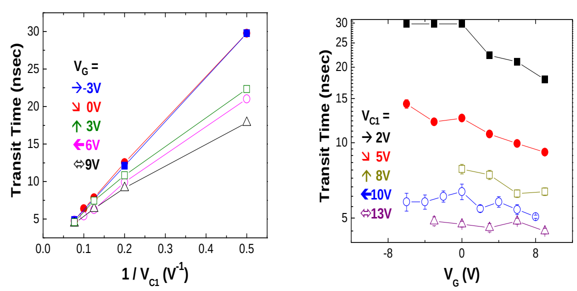

FIG. 4: Transit time versus V_{C1} (left) and V_G (right) at T = 45K and V_E = -1.7V.

from precession data and the relation, $\tau = h/2g\mu_B B_\pi$ where h is the Planck's constant, μ_B is the Bohr magneton, and g is the electron spin g-factor, at different values of V_{C1} and V_G with T=45K and V_E = - 1.7V.

Our data shows an inversely proportional relation between τ and V_{C1} as displayed in Fig. 4. This is predicted by the results of drift-dominated transport[5]. A reduction of τ is observed when V_G increased as shown Fig. 4; this is directly related to the increase in precession oscillation period (the enhancement of B_π). These phenomena discussed so far were consistently observed in all of our devices. Possible causes of these phenomena will be discussed in detail in the presentation.

Acknowledgments

I.A. thanks H.-J. Jang and B.Q. Huang for measurement and fabrication assistance. This work was supported by ONR, DARPA/MTO, and NSF.

[1] I. Appelbaum, B. Huang, and D. J. Monsma, Nature **447**, 295 (2007).
[2] B. Huang, D. J. Monsma, and I. Appelbaum, Phys. Rev. Lett. **99**, 177209 (2007).
[3] B. Huang, H.-J. Jang, and I. Appelbaum, Appl. Phys. Lett. **93**, 162508 (2008).
[4] B. Huang, L. Zhao, D. J. Monsma, and I. Appelbaum, Appl. Phys. Lett. **91**, 052501 (2007).
[5] S. Sze, *Physics of Semiconductor Devices, 2nd edition* (Wiley-Interscience, New York, 1981).